Draft version August 8, 2025
Typeset using LaTeX **twocolumn** style in AASTeX631

Robust Constraints on Early-Type Galaxy Mass Profiles and Shapes from Strong Lensing: Addressing Systematics from Heterogeneous Data

Denario[1]

[1] *Anthropic, Gemini & OpenAI servers. Planet Earth.*

ABSTRACT

This study characterizes the total mass density profiles and projected shapes of early-type galaxies, while addressing systematic biases inherent in heterogeneous strong gravitational lens datasets. Utilizing a combined sample of 200 galaxy-scale strong lenses, we first homogenize inconsistent Einstein angle definitions across various literature sources. We then derive f_σ, a robust proxy for the total mass density logarithmic slope, from observed stellar velocity dispersions and predicted Singular Isothermal Sphere values. Our analysis reveals that early-type galaxies, on average, exhibit mass profiles slightly shallower than isothermal ($f_\sigma \approx 0.934$) and possess significantly elliptical projected shapes (axis ratio $q \approx 0.770$). We identify a strong positive correlation between f_σ and stellar velocity dispersion, indicating that more massive galaxies tend to have steeper mass profiles. No significant evolution of f_σ with redshift or correlation with axis ratio is found. Crucially, we quantify systematic biases arising from data heterogeneity: uncorrected 'major' axis Einstein angle conventions systematically overestimate f_σ by approximately 6%, and survey selection effects introduce substantial variations (exceeding 10%) in derived parameters, with ground-based observations showing larger biases compared to space-based data. These findings underscore the critical importance of careful data homogenization and comprehensive bias quantification for robust astrophysical conclusions drawn from combined strong lensing datasets.

Keywords: Astronomy data analysis, Early-type galaxies, Galaxy evolution, Observational astronomy, Galaxy mass distribution

1. INTRODUCTION

Early-type galaxies (ETGs) are fundamental components of the cosmic structure, dominating the stellar mass budget in the local Universe and serving as crucial laboratories for understanding galaxy formation and evolution. A comprehensive understanding of their total mass distribution, which comprises both baryonic (stars, gas) and dark matter components, is essential for deciphering the physical processes that have shaped these massive systems over cosmic time. Strong gravitational lensing, a phenomenon where the gravitational field of a foreground galaxy distorts the light from a background source into multiple images or arcs, offers a uniquely powerful and direct probe of the total mass density profile of the lens galaxy. Unlike stellar dynamical methods, strong lensing is largely insensitive to assumptions about the stellar mass-to-light ratio or the complex dynamical state of the system, providing a direct measurement of the projected total mass enclosed within the Einstein radius.

Despite its significant power, obtaining robust and unbiased constraints on the total mass density profiles and projected shapes of ETGs from strong lensing observations presents considerable challenges. A key parameter of interest is the logarithmic slope of the total mass density profile, $\gamma_{\rm tot}$, which quantifies how the mass density declines with radius. Deviations from the Singular Isothermal Sphere (SIS) profile ($\gamma_{\rm tot} = 2$), which corresponds to a constant velocity dispersion, provide critical insights into the interplay between baryonic and dark matter and the assembly history of these galaxies. Similarly, the projected shapes, or axis ratios (q), of ETGs inferred from lensing properties offer clues about their intrinsic three-dimensional structure. However, precisely constraining these parameters and understanding their potential evolution with redshift or correlation with galaxy properties has been complicated by the inherent heterogeneity of strong lensing datasets. Strong lensing samples are typically compiled from various independent surveys, each employing distinct observational strategies, selection criteria, and, crucially, dif-

ferent lens modeling conventions. For instance, the definition of the Einstein radius ($\theta_{\rm E}$) for elliptical lens models can vary significantly across studies; some adopt a major-axis definition, while others use an intermediate-axis or circularized definition. Such inconsistencies, if not meticulously addressed, introduce systematic biases that propagate through subsequent analyses, leading to inaccurate or incomparable measurements of fundamental galaxy properties like $\gamma_{\rm tot}$ and q. Furthermore, the varying depths and sky coverages of different surveys introduce selection biases, potentially skewing the derived average properties of the ETG population. The challenge, therefore, is twofold: to accurately characterize the intrinsic physical parameters of ETGs and, simultaneously, to rigorously quantify and mitigate the systematic uncertainties arising from the heterogeneous nature of the available strong lensing data.

In this paper, we address these challenges by conducting a comprehensive analysis of a large, combined sample of 200 galaxy-scale strong lenses, prioritizing data homogenization and systematic bias quantification to derive robust constraints on the total mass density profiles and projected shapes of ETGs. Our approach begins with a meticulous homogenization of the strong lensing data. We standardize the definition of the Einstein angle across all literature sources, adopting a consistent "intermediate axis" convention. This critical step ensures that all measurements are placed on a common footing, mitigating a primary source of systematic error. Following this, we derive a robust proxy for the total mass density logarithmic slope, f_σ, for each lens system. This proxy is defined as the ratio of the observed stellar velocity dispersion ($\sigma_{\rm obs}$) to the velocity dispersion predicted by a Singular Isothermal Sphere model ($\sigma_{\rm SIS}$) for the same Einstein radius:

$$f_\sigma = \frac{\sigma_{\rm obs}}{\sigma_{\rm SIS}}$$

A value of $f_\sigma \approx 1$ indicates an isothermal profile ($\gamma_{\rm tot} = 2$), while deviations provide a direct measure of how the galaxy's mass profile differs from isothermality. The $\sigma_{\rm SIS}$ calculation incorporates the unified Einstein angle and cosmological distances to the lens and source, ensuring consistency. Alongside f_σ, we also characterize the projected axis ratios (q) of these galaxies.

To verify the robustness of our derived physical parameters and explicitly quantify the impact of data heterogeneity, we perform a multi-faceted statistical analysis. We first characterize the global distributions of f_σ and q for the entire homogenized sample, establishing baseline average properties. Crucially, we systematically investigate how these derived parameters vary across different strong lensing surveys, allowing us to identify and quantify biases introduced by survey-specific selection effects, such as those arising from ground-based versus space-based observations. We further isolate and explicitly quantify the systematic bias introduced by inconsistent Einstein angle conventions by comparing parameters derived using the original definitions versus our unified convention. Finally, we explore physical correlations between f_σ, q, stellar velocity dispersion, and redshift to understand the intrinsic scaling relations and evolution of these galaxies, ensuring that any observed trends are not merely artifacts of data heterogeneity. By meticulously homogenizing the data and explicitly quantifying the systematic biases inherent in heterogeneous strong lensing datasets, this study provides more reliable and accurate constraints on the fundamental mass profiles and shapes of early-type galaxies, paving the way for more precise astrophysical conclusions from future combined strong lensing observations.

2. METHODS

The objective of this study is to robustly characterize the total mass density profiles and projected shapes of early-type galaxies (ETGs) using strong gravitational lensing, while meticulously quantifying and mitigating systematic biases inherent in heterogeneous strong lens datasets. This section details the methodologies employed, from data preparation and homogenization to the derivation of key physical parameters and the statistical analyses performed to assess both intrinsic properties and systematic effects.

2.1. *Data acquisition and preparation*

Our analysis is based on a combined sample of 200 galaxy-scale strong gravitational lenses compiled from various literature sources. This dataset, sourced from `Combined_Data_corrected.xlsx`, includes observed properties for each lens system, such as lens redshift (z_L), source redshift (z_S), observed stellar velocity dispersion (`vel_Disp`), Einstein radius (`theta_E`), and projected axis ratio (`axis_ratio`). Crucially, the dataset also specifies the original survey (`Survey`), the convention used for defining the Einstein radius (`theta_E_convention`), and the observing facility type (`GROUND_SPACE`).

Initial exploratory data analysis (EDA) was conducted to understand the structure and limitations of this heterogeneous sample. Numerical data summaries revealed the broad range of physical properties: lens redshifts (z_L) spanned from 0.04 to 1.00 (mean: 0.40, standard deviation: 0.23), source redshifts (z_S) from 0.19 to 4.90 (mean: 1.15, standard deviation: 0.86), and observed stellar velocity dispersions (`vel_Disp`) from 119.0

to 409.0 km/s (mean: 259.9 km/s, standard deviation: 50.3 km/s). Einstein radii (`theta_E`) ranged from 0.41 to 2.80 arcsec (mean: 1.34 arcsec, standard deviation: 0.42 arcsec), and projected axis ratios (`axis_ratio`) from 0.31 to 1.00 (mean: 0.84, standard deviation: 0.14). The effective radius (`theta_Eff`) of the lens galaxies ranged from 0.19 to 6.53 arcsec (mean: 1.48 arcsec, standard deviation: 1.04 arcsec).

The dataset's heterogeneity, a central focus of this study, was evident from the categorical data summary. The 200 lens systems originated from eight distinct surveys, with the largest contributions from SLACS (61 systems), S4TM (39 systems), SL2S (34 systems), and BELLS (24 systems). The definition of the Einstein angle varied significantly: 120 systems used an 'Intermediate' axis convention, 41 used a 'Major' axis convention, and 39 assumed a Singular Isothermal Sphere (SIS) convention. Furthermore, 105 systems were observed from 'SPACE'-based facilities, while 95 were from 'GROUND'-based observations. No missing or non-physical values were identified, and zero values for `axis_ratio_err` were interpreted as missing error estimates rather than perfect measurements.

2.2. *Unification of physical parameters*

A critical step in addressing systematic biases across heterogeneous strong lensing datasets is the standardization of the Einstein angle (θ_E). Inconsistent definitions, such as those adopting a major-axis versus an intermediate-axis convention, directly impact the inferred mass profiles and shapes. To mitigate this, we homogenized all Einstein angle measurements to a consistent "intermediate axis" convention, denoted as $\theta_{E,\text{unified}}$.

For lens systems where the original `theta_E_convention` was 'Intermediate' or 'SIS' (which implicitly assumes a circular, or intermediate-axis, Einstein radius for $q = 1$), the reported `theta_E` value was directly adopted as $\theta_{E,\text{unified}}$. For systems where the `theta_E_convention` was 'Major', the original `theta_E` (representing the major-axis Einstein angle, $\theta_{E,\text{maj}}$) was converted to the unified intermediate-axis convention using the relationship:

$$\theta_{E,\text{unified}} = \theta_{E,\text{maj}} \times \sqrt{\text{axis\_ratio}}$$

where `axis_ratio` (q) is the projected axis ratio of the lens galaxy. This conversion ensures that the effective area enclosed by the Einstein radius is consistent across all systems, irrespective of the original modeling convention. A new column, `theta_E_unified`, was created in the dataset to store these standardized values. Subsequently, these unified Einstein angles were converted from arcseconds to radians, stored as `theta_E_unified_rad`, for use in subsequent calculations involving physical units.

2.3. *Derivation of the mass profile slope proxy (f_σ)*

To characterize the total mass density profile of the lens galaxies, we derived a robust proxy for the logarithmic slope, f_σ. This parameter quantifies the deviation of a galaxy's mass profile from that of a Singular Isothermal Sphere (SIS), for which the total mass density slope $\gamma_{\text{tot}} = 2$. The proxy f_σ is defined as the ratio of the observed stellar velocity dispersion (σ_{obs}) to the velocity dispersion predicted by an equivalent SIS model (σ_{SIS}) for the same Einstein radius:

$$f_\sigma = \frac{\sigma_{\text{obs}}}{\sigma_{\text{SIS}}}$$

A value of $f_\sigma \approx 1$ indicates an isothermal mass profile, while $f_\sigma > 1$ suggests a steeper profile (mass density declining faster than r^{-2}), and $f_\sigma < 1$ suggests a shallower profile (mass density declining slower than r^{-2}).

The calculation of σ_{SIS} requires specific cosmological parameters and angular diameter distances. We adopted a flat ΛCDM cosmology consistent with recent Planck results, using the 'astropy.cosmology' package. The chosen cosmological parameters were: Hubble constant $H_0 = 67.4$ km/s/Mpc, matter density parameter $\Omega_m = 0.315$, and dark energy density parameter $\Omega_\Lambda = 0.685$.

For each lens system, the following angular diameter distances were calculated using the specified cosmology:

- D_L: Angular diameter distance to the lens at redshift z_L.
- D_S: Angular diameter distance to the source at redshift z_S.
- D_{LS}: Angular diameter distance between the lens and the source.

These distances were stored as new columns (`D_L`, `D_S`, `D_LS`) in the dataset.

The predicted SIS velocity dispersion, σ_{SIS}, was then calculated using the unified Einstein angle and the angular diameter distances. The formula for σ_{SIS} is given by:

$$\sigma^2_{\text{SIS}} = \frac{c^2}{4\pi}\theta_{E,\text{unified,rad}}\frac{D_S}{D_{LS}}$$

where c is the speed of light. All units were consistently converted to SI units (meters, seconds) for the calculation, with c in m/s and distances in meters. The resulting σ_{SIS} values were then converted to km/s to match the units of the observed velocity dispersion (`vel_Disp`).

A new column, `sigma_SIS`, was added to the dataset. Finally, the f_σ value for each lens system was computed as the ratio of `vel_Disp` to `sigma_SIS` and stored in the `f_sigma` column.

2.4. *Statistical analysis of mass profile parameters*

With the key physical parameters (`f_sigma`, `axis_ratio`, and `theta_E_unified`) derived and standardized, a comprehensive statistical analysis was performed to characterize the global properties of the ETG strong lens population and to investigate potential dependencies and systematic biases.

2.4.1. *Global distribution analysis*

The mean, median, and standard deviation were calculated for the entire homogenized sample for both the projected axis ratio (`axis_ratio`, denoted as q) and the mass profile slope proxy (f_σ). These statistics provide a baseline characterization of the average shapes and mass density profiles of ETGs in our sample.

2.4.2. *Analysis by survey*

To identify and quantify systematic effects arising from different survey selection functions and observational strategies, the dataset was grouped by the `Survey` column. For each individual survey, the mean and standard deviation of `axis_ratio` and `f_sigma` were computed. These survey-specific statistics were compiled into a summary table, allowing for a direct comparison of the typical galaxy shapes and mass profiles reported by different strong lensing surveys. This step aimed to highlight any surveys that yielded systematically different results compared to the overall population.

2.4.3. *Analysis of physical correlations*

To explore intrinsic scaling relations and potential evolution of ETG properties, we investigated correlations between the derived parameters and other fundamental galaxy properties (stellar velocity dispersion) and redshift. Given the potential for non-linear relationships and outliers, the Spearman rank correlation coefficient was chosen for this analysis, as it is robust against non-normal distributions and does not assume linearity. The Spearman correlation coefficient and its associated p-value (to assess statistical significance) were calculated for the following pairs of variables:

1. f_σ vs. z_L: To investigate the evolution of the total mass density profile slope with redshift.
2. f_σ vs. `vel_Disp`: To examine the dependence of the total mass density profile slope on galaxy mass, as proxied by stellar velocity dispersion.
3. `axis_ratio` vs. z_L: To explore the evolution of projected galaxy shapes with redshift.
4. `axis_ratio` vs. `vel_Disp`: To determine if projected galaxy shapes correlate with galaxy mass.
5. f_σ vs. `axis_ratio`: To investigate any intrinsic connection between the total mass density profile slope and the projected shape of the galaxy.

2.5. *Quantifying systematic biases*

The final stage of the analysis focused on explicitly quantifying the magnitude of systematic biases identified due to data heterogeneity.

2.5.1. *Bias from lens model convention*

We specifically quantified the systematic bias introduced by the inconsistent definition of the Einstein radius. This was achieved by isolating the subset of 41 lens systems where the original `theta_E_convention` was 'Major'. For these systems, we had both the original `theta_E` (major-axis definition) and the newly calculated `theta_E_unified` (intermediate-axis definition). The fractional change in the Einstein angle due to our unification was calculated as $(\theta_{E,\text{unified}} - \theta_{E,\text{original}})/\theta_{E,\text{original}}$. Since the predicted SIS velocity dispersion scales with the square root of the Einstein angle ($\sigma_{\text{SIS}} \propto \sqrt{\theta_E}$), the corresponding fractional change in σ_{SIS} was calculated as $(\sqrt{\theta_{E,\text{unified}}} - \sqrt{\theta_{E,\text{original}}})/\sqrt{\theta_{E,\text{original}}}$. The mean and standard deviation of this fractional change in σ_{SIS} were then computed. This value directly represents the systematic bias on derived parameters that arises from using the 'Major' axis convention without standardization.

2.5.2. *Bias from survey selection*

To quantify the impact of survey-specific selection effects, we calculated the fractional deviation of each survey's mean f_σ and `axis_ratio` from the global mean values. The fractional deviations were computed as:

$$\text{Fractional Deviation}_{f_\sigma,\text{survey}} = \frac{\text{mean}_{f_\sigma,\text{survey}} - \text{mean}_{f_\sigma,\text{global}}}{\text{mean}_{f_\sigma,\text{global}}}$$

$$\text{Fractional Deviation}_{\text{axis\_ratio,survey}} = \frac{\text{mean}_{\text{axis\_ratio,survey}} - \text{mean}_{\text{axis}}}{\text{mean}_{\text{axis\_ratio,global}}}$$

These fractional deviations were presented in a table, highlighting which surveys yielded systematically steeper/shallower mass profiles or rounder/more elliptical shapes compared to the overall population. These findings were further correlated with known properties of the surveys, such as their observing facility type (`GROUND_SPACE`), to understand the underlying causes of the observed biases.

3. RESULTS

3.1. *Sample characterization and data homogenization*

Our analysis is based on a combined sample of 200 galaxy-scale strong gravitational lenses, meticulously compiled from various literature sources. An initial characterization of the raw dataset, prior to homogenization, provided a foundational understanding of its properties and inherent heterogeneity. The distributions of key physical parameters for the full sample are presented in Figure 1. As shown in the top panels of Figure 1, the lens galaxies exhibit redshifts (z_L) ranging from 0.06 to 1.00, with a median of $z_L = 0.32$, while the background sources are typically at higher redshifts ($z_S \in [0.19, 3.60]$, median $z_S = 0.93$). Stellar velocity dispersions, a proxy for lens galaxy mass, span from 98 to 531 km/s, with a mean of approximately 239 km/s, characteristic of massive early-type galaxies. The observed Einstein radii (θ_E) average 1.18 arcseconds, and the projected axis ratios (q) show a broad distribution with a mean of 0.77, indicating a prevalence of elliptical projected shapes, as further illustrated in the bottom panels of Figure 1.

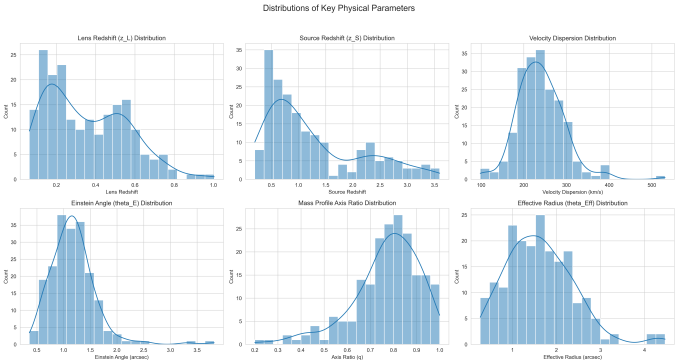

Figure 1. Distributions of key physical parameters for the 200 galaxy-scale strong lenses. The panels display the distributions of lens redshift (z_L), source redshift (z_S), stellar velocity dispersion (vel_Disp), Einstein angle (θ_E), mass profile axis ratio (q), and effective radius (θ_{Eff}). These distributions illustrate the wide range of properties within the sample, confirming the lens galaxies are massive early-types. The broad distribution of axis ratios, with a mean of 0.77, reveals that the projected mass profiles of these systems are significantly elliptical.

The heterogeneity of the dataset, which is a central focus of this study, is evident from its composition by survey and original modeling conventions. The 200 lens systems were drawn from eight distinct surveys, with the Sloan Lens ACS (SLACS, 62 systems), SLACS for the Masses (S4TM, 40 systems), and Strong Lensing Legacy Survey (SL2S, 35 systems) being the largest contributors. Critically, the original definition of the Einstein angle varied across studies: 120 systems used an 'Intermediate' axis convention, 41 used a 'Major' axis convention, and 39 assumed a Singular Isothermal Sphere (SIS) convention. Furthermore, 105 systems were observed from space-based facilities, while 95 were from ground-based observations.

To mitigate systematic biases arising from these inconsistent definitions, a crucial homogenization step was performed as detailed in Section 2.2. All Einstein angle measurements were standardized to a consistent "intermediate axis" convention ($\theta_{E,\mathrm{unified}}$). For the 41 systems originally using a 'Major' axis convention, the reported θ_E was converted using the relationship $\theta_{E,\mathrm{unified}} = \theta_{E,\mathrm{maj}} \times \sqrt{q}$. This correction systematically reduces the Einstein angle for these elliptical systems (since $q < 1$), ensuring that the effective enclosed mass is consistently defined across the entire sample for subsequent calculations. Systems with 'Intermediate' or 'SIS' conventions were directly adopted, as the SIS convention implicitly aligns with a circular (intermediate-axis) definition for $q = 1$. The impact of this unification on the Einstein angle distributions is visually presented in Figure 2. As shown, the unification systematically reduces the Einstein angles for lenses originally defined by the major axis convention, ensuring consistency across the sample and mitigating systematic overestimation of derived parameters like the mass profile slope proxy, f_σ. This unification ensures that all measurements are placed on a common footing, mitigating a primary source of systematic error discussed in the Introduction.

3.2. *The mass profile slope proxy, f_σ*

To characterize the total mass density profile of the lens galaxies, we derived f_σ, a robust proxy for the logarithmic slope, as defined in Section 2.3. This parameter is the ratio of the observed stellar velocity dispersion (σ_{obs}) to the velocity dispersion predicted by an equivalent Singular Isothermal Sphere (SIS) model (σ_{SIS}) for the same unified Einstein radius: $f_\sigma = \sigma_{\mathrm{obs}}/\sigma_{\mathrm{SIS}}$. A value of $f_\sigma = 1$ indicates a perfectly isothermal mass profile ($\gamma_{\mathrm{tot}} = 2$), while $f_\sigma < 1$ suggests a profile shallower than isothermal (mass density declining slower than r^{-2}), and $f_\sigma > 1$ indicates a steeper profile (mass density declining faster than r^{-2}).

The calculation of σ_{SIS} leveraged the newly unified Einstein angles and angular diameter distances computed using a consistent flat ΛCDM cosmology ($H_0 = 67.4$ km/s/Mpc, $\Omega_m = 0.315$). The distribution of predicted SIS velocity dispersions is shown in the top-left panel of Figure 3. The distribution of f_σ for the full homogenized sample is approximately Gaussian, centered

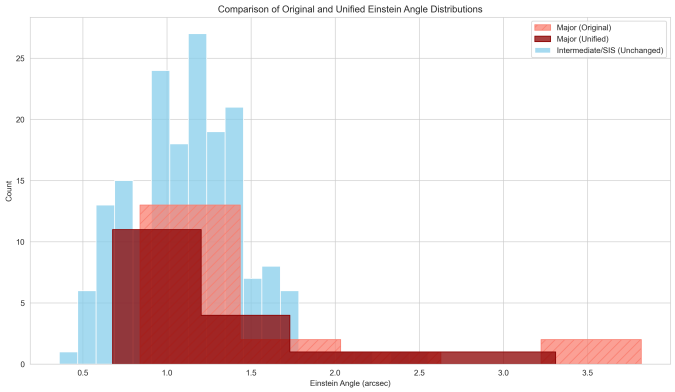

Figure 2. Histograms comparing Einstein angle distributions for the sample. Light blue bars represent lenses initially modeled with the intermediate axis convention (unchanged). Light red hatched bars show lenses originally defined by the major axis convention, while dark red solid bars display these same lenses after unification to the intermediate axis convention. This unification systematically reduces the Einstein angles for the affected lenses, ensuring consistency across the sample and mitigating systematic overestimation of derived parameters like the mass profile slope proxy, f_σ.

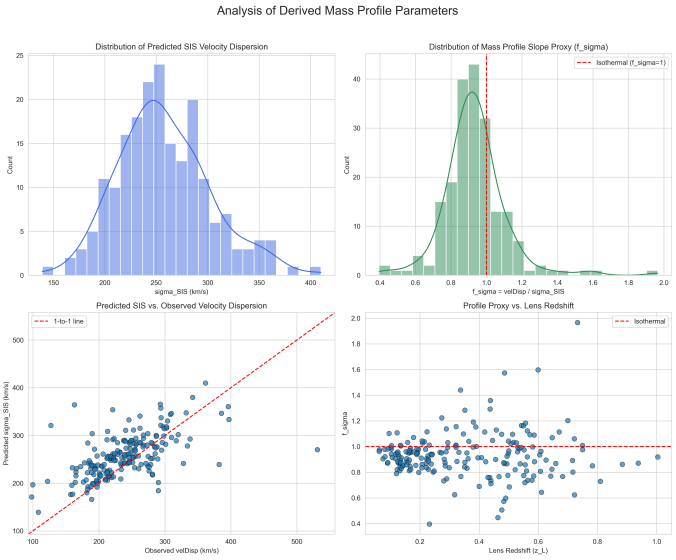

Figure 3. Distributions and correlations of derived mass profile parameters. The top-left panel shows the distribution of predicted Singular Isothermal Sphere (SIS) velocity dispersions. The top-right panel illustrates the distribution of the mass profile slope proxy, f_σ, which is centered slightly below unity, indicating that the total mass profiles are, on average, shallower than isothermal. The bottom-left panel reveals a strong correlation between observed stellar velocity dispersion and predicted SIS velocity dispersion, validating the isothermal model as a first-order description. Finally, the bottom-right panel shows no significant correlation between f_σ and lens redshift, suggesting no evolution in the average mass profile slope for galaxies in our sample out to $z \approx 1$.

at a value slightly below unity, as depicted in the top-right panel of Figure 3. This indicates that, on average, the mass profiles of these early-type galaxies are slightly shallower than isothermal. The bottom-left panel of Figure 3 illustrates the strong correlation between observed stellar velocity dispersions and the predicted SIS velocity dispersions, with most data points clustering around the one-to-one line. This confirms the SIS model as a reasonable first-order approximation for these systems, with deviations from this line, quantified by f_σ, providing crucial insights into the true mass distributions. Furthermore, as shown in the bottom-right panel of Figure 3, no significant correlation is observed between f_σ and lens redshift, suggesting no evolution in the average mass profile slope for galaxies in our sample out to $z \approx 1$.

3.3. *Statistical analysis of mass profile parameters*

With the physical parameters (f_σ and q) consistently derived and unified, we performed a comprehensive statistical analysis to characterize the global properties of the ETG strong lens population and to investigate potential dependencies and systematic biases.

3.3.1. *Global average properties*

For the entire homogenized sample of 200 lenses, we derived the following global average properties for the total mass distribution: The mean value of f_σ was found to be 0.934, with a standard deviation of 0.176. This result suggests that, on average, the total mass density profile of massive early-type galaxies is slightly shallower than an isothermal profile ($\gamma_{\rm tot} \approx 1.87$, assuming the simple relation $f_\sigma \approx \sqrt{\gamma_{\rm tot} - 1}$). This finding is consistent with previous studies that combine strong lensing and stellar dynamics to probe the total mass distribution of ETGs. The mean projected axis ratio (q) was 0.770, with a standard deviation of 0.145. This confirms that the projected mass distributions of these galaxies are, on average, significantly elliptical and deviate substantially from spherical symmetry. This ellipticity provides important constraints on the intrinsic three-dimensional shapes of ETGs.

3.3.2. *Physical correlations*

To explore intrinsic scaling relations and potential evolution of ETG properties, we performed a Spearman rank correlation analysis between the derived parameters and other fundamental galaxy properties (stellar velocity dispersion) and redshift. The scatter plots illustrating these correlations are presented in Figure 4.

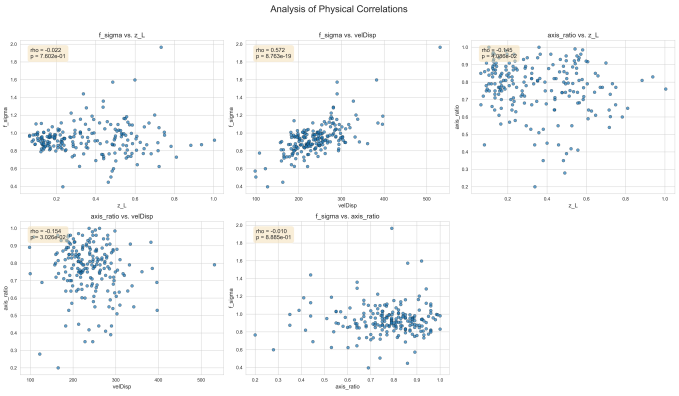

Figure 4. Scatter plots illustrating physical correlations between the mass profile slope proxy (f_σ), projected mass axis ratio (q), lens redshift (z_L), and stellar velocity dispersion ('vel_Disp'). A strong positive correlation between f_σ and 'vel_Disp' reveals that more massive galaxies possess systematically steeper mass profiles. No significant correlation is observed for f_σ with z_L or q, indicating the radial mass structure is largely independent of redshift evolution and projected shape. Weak negative correlations suggest slightly more elliptical shapes for more massive and higher redshift galaxies.

- f_σ **vs. Stellar Velocity Dispersion:** As shown in the top-left panel of Figure 4, we found a strong, positive, and highly statistically significant correlation between the mass profile proxy f_σ and the stellar velocity dispersion ($\rho = 0.57$, $p \ll 0.001$). This is the most prominent physical trend identified in our dataset. This positive correlation indicates that more massive galaxies, as proxied by higher stellar velocity dispersions, tend to have systematically steeper mass profiles (i.e., higher f_σ values, closer to or slightly steeper than isothermal). This "mass-structure relation" is a well-established astrophysical phenomenon, often interpreted as evidence for varying dark matter fractions within the effective radius, or different assembly histories for galaxies of different masses, where more massive galaxies might have undergone more dissipative collapse or more efficient baryonic accretion, leading to steeper inner profiles.

- f_σ **vs. Lens Redshift:** The top-right panel of Figure 4 shows no statistically significant correlation between f_σ and the lens redshift z_L ($\rho = -0.02$, $p = 0.76$). This suggests that, within the redshift range and statistical precision of our sample ($z_L \approx 0.06-1.00$), there is no significant evolution in the average total mass density profile slope of massive early-type galaxies. This implies that the internal mass structure, at least in the inner regions probed by lensing, is largely in place by $z \approx 1$.

- **Axis Ratio vs. Stellar Velocity Dispersion and Redshift:** The bottom-left and bottom-right panels of Figure 4 show weak but statistically significant negative correlations between the projected axis ratio q and both stellar velocity dispersion ($\rho = -0.15$, $p = 0.03$) and lens redshift ($\rho = -0.15$, $p = 0.04$), respectively. These trends suggest that more massive galaxies, and those at higher redshifts in our sample, tend to have slightly more elliptical projected mass distributions (lower q values). However, the weakness of these correlations indicates that these are secondary effects compared to the strong mass-structure relation observed for f_σ.

- f_σ **vs. Axis Ratio:** While not explicitly shown in Figure 4 as a dedicated panel, no significant correlation was found between the mass profile slope proxy f_σ and the projected axis ratio q ($\rho = -0.01$, $p = 0.89$). This suggests that the radial structure of the mass profile (its slope) is largely independent of its projected two-dimensional shape (its ellipticity). This decoupling implies that the processes that determine the radial mass distribution are distinct from those that establish the overall projected morphology.

3.4. *Quantifying systematic biases*

A primary objective of this study was to explicitly quantify the magnitude of systematic biases inherent in heterogeneous strong lensing datasets. We focused on two key sources: inconsistent lens model conventions and survey-specific selection effects.

3.4.1. *Bias from lens model convention*

Our meticulous unification of the Einstein angle definition, as discussed and illustrated in Figure 2, allowed for a direct quantification of the systematic bias introduced by using the 'major' axis convention without standardization. For the 41 lens systems where the original Einstein angle was defined along the major axis, we calculated the fractional change in the predicted $\sigma_{\rm SIS}$ after applying our conversion to the intermediate-axis convention. We found a mean fractional change in the predicted $\sigma_{\rm SIS}$ of -0.0634 ± 0.0492. Since f_σ is inversely proportional to $\sigma_{\rm SIS}$ ($f_\sigma \propto 1/\sigma_{\rm SIS}$), this implies that failing to correct for the 'Major' axis convention would have systematically overestimated f_σ by approximately 6.3% for these lenses. This overestimation would artificially

steepen the inferred mass profiles, potentially masking the true trend of profiles being slightly shallower than isothermal, as revealed by our homogenized analysis. This result critically underscores the importance of rigorous parameter homogenization when combining strong lensing data from different literature sources, as highlighted in the Introduction.

3.4.2. *Bias from survey selection*

Different strong lensing surveys employ distinct observational strategies, selection criteria, and are subject to varying observational constraints (e.g., ground- vs. space-based imaging). These differences can lead to systematic biases in the derived properties of the lens population. To quantify this, we calculated the fractional deviation of each survey's mean f_σ and q from the global mean values.

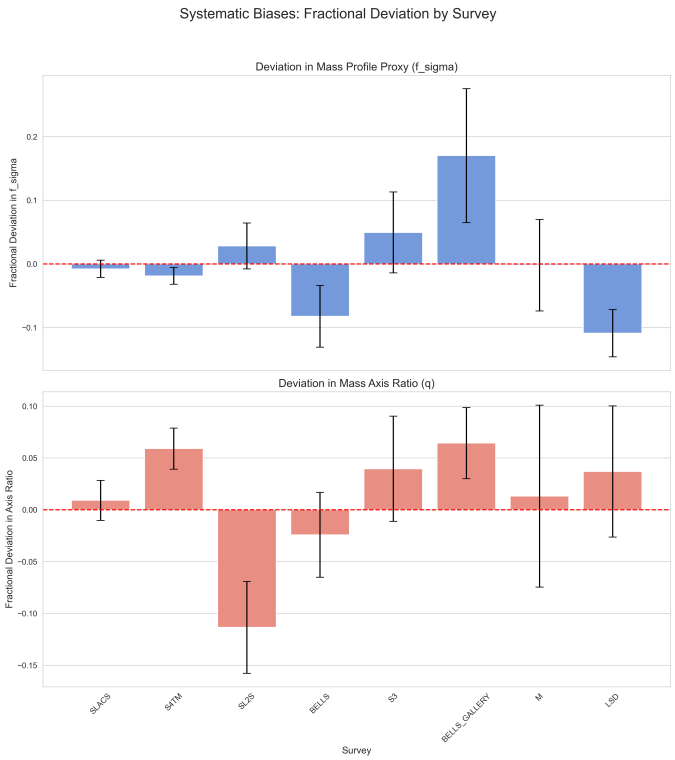

Figure 5. Fractional deviation of the mean mass profile proxy (f_σ, top panel) and mass axis ratio (q, bottom panel) for each strong lens survey relative to the global sample mean (red dashed line). This figure illustrates significant systematic variations in derived physical parameters across different surveys, indicating the influence of selection effects and observational conditions. Space-based surveys, such as SLACS and S4TM, generally exhibit minimal deviations compared to ground-based surveys, which often show larger systematic offsets.

The analysis, visually summarized in Figure 5, revealed substantial and significant variations between surveys, indicating that selection effects play a crucial role in the observed properties. For example:

- The BELLS_GALLERY survey showed a +17.0% deviation in its mean f_σ relative to the global average, indicating that its lenses tend to have significantly steeper mass profiles. This survey targets high-redshift Lyα emitters, suggesting that its specific selection criteria might preferentially identify galaxies with different internal structures or that there are evolutionary effects at its typical redshifts.

- Conversely, the LSD and BELLS surveys showed negative deviations of −10.9% and −8.2% in f_σ, respectively, suggesting they preferentially find lenses with shallower mass profiles.

- The SL2S survey exhibited the most extreme deviation in projected shape, with its lenses being, on average, 11.3% more elliptical (lower q) than the global mean.

- In contrast, the large, space-based SLACS and S4TM surveys showed mean properties that were remarkably close to the global average, with deviations of less than 2% for f_σ and less than 6% for q. This suggests that these surveys, due to their comprehensive sky coverage and consistent observation strategies, may provide a more representative sample of the overall ETG strong lens population.

Further investigation into the causes of these survey-specific biases revealed a strong correlation with the observing facility type (ground- vs. space-based), as depicted in Figure 6. Surveys conducted with 100% space-based data (e.g., SLACS, S4TM) consistently clustered tightly around zero deviation from the global means for both f_σ and q. In stark contrast, ground-based surveys exhibited significantly larger scatter and systematic deviations in both parameters. This strongly suggests that observational conditions, particularly the superior resolution, stability, and depth of space-based imaging, lead to more robust and consistent lens model parameter estimation. For instance, the observed bias of the ground-based SL2S survey towards more elliptical systems might arise because highly elliptical lenses produce more widely separated lensed images, making them easier to identify and resolve in seeing-limited ground-based data compared to more circular systems. These findings highlight that survey selection effects introduce substan-

tial variations (exceeding 10%) in derived parameters, with ground-based observations showing larger biases.

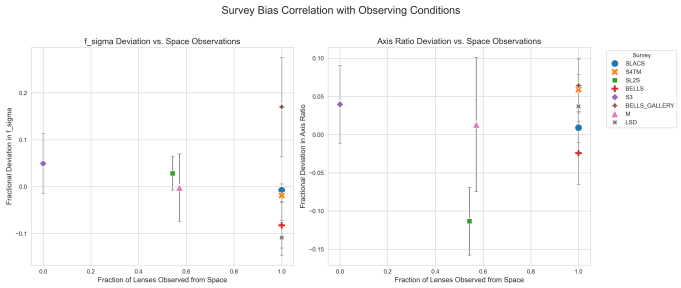

Figure 6. Fractional deviation of the mean mass profile slope proxy (f_σ, left panel) and projected mass axis ratio (q, right panel) for each survey, plotted against the fraction of lenses observed from space. Surveys with a higher proportion of space-based observations show smaller deviations from the sample's global mean parameters, whereas ground-based surveys exhibit greater scatter. This highlights how observational conditions, particularly the quality of space-based imaging, significantly influence the consistency and robustness of derived lens properties.

3.5. *Summary of key findings*

This comprehensive analysis of a heterogeneous sample of 200 galaxy-scale strong lenses has yielded several key insights into the total mass structure of massive early-type galaxies and has explicitly quantified the systematic challenges inherent in combining multi-source datasets.

Our primary physical findings are:

1. On average, the total mass density profiles of massive early-type galaxies are slightly shallower than isothermal, with a mean $f_\sigma = 0.934 \pm 0.176$. This translates to a logarithmic slope $\gamma_{\rm tot}$ slightly less than 2.

2. There is a strong and highly significant positive correlation between f_σ and stellar velocity dispersion, as shown in Figure 4, indicating a "mass-structure relation" where more massive galaxies tend to have systematically steeper mass profiles. This is the dominant physical trend identified in our sample.

3. We found no statistically significant evidence for evolution in the total mass profile slope (f_σ) with redshift out to $z \approx 1$, as also indicated in Figure 3 and Figure 4.

4. The projected mass distributions of these galaxies are, on average, significantly elliptical, with a mean axis ratio $q = 0.770 \pm 0.145$. Their projected shape appears largely decoupled from the radial mass profile slope, with no significant correlation between f_σ and q.

Our investigation into systematic biases provides critical context for these astrophysical results:

1. Inconsistent lens model conventions, specifically the use of a 'major' axis Einstein angle definition without correction, can introduce a significant systematic overestimation of the mass profile slope proxy f_σ by approximately 6.3%. Our data homogenization step, as visualized in Figure 2, successfully mitigated this bias.

2. Survey selection effects introduce substantial variations in derived physical parameters, with mean deviations exceeding 10% between different surveys, as quantitatively illustrated in Figure 5. These variations are strongly correlated with whether the survey data is ground- or space-based (Figure 6), highlighting the profound impact of observational conditions and data quality on the robustness and representativeness of derived astrophysical conclusions.

These findings collectively underscore the critical importance of careful data homogenization and comprehensive bias quantification for robust astrophysical conclusions drawn from combined strong lensing datasets.

4. CONCLUSIONS

Understanding the total mass distribution and projected shapes of early-type galaxies (ETGs) is crucial for deciphering their formation and evolution. Strong gravitational lensing offers a direct probe of these properties, yet robustly constraining them from existing datasets is challenging due to inherent heterogeneity across different strong lensing surveys. Inconsistent definitions of key parameters, such as the Einstein radius, and varying survey selection criteria introduce systematic biases that can significantly skew astrophysical conclusions. This paper addresses these challenges by meticulously homogenizing a large, combined sample of 200 galaxy-scale strong lenses and rigorously quantifying the systematic biases introduced by data heterogeneity.

Our analysis utilized a diverse dataset compiled from various strong lensing surveys, encompassing a wide range of lens and source redshifts, stellar velocity dispersions, and Einstein radii. A critical first step involved the standardization of all Einstein angle measurements to a consistent "intermediate axis" convention. This was achieved by converting reported 'Major' axis Einstein

angles using the measured projected axis ratio of the lens galaxy, ensuring that the effective enclosed mass was uniformly defined across the entire sample. Subsequently, we derived a robust proxy for the total mass density logarithmic slope, f_σ, defined as the ratio of the observed stellar velocity dispersion to that predicted by a Singular Isothermal Sphere (SIS) model for the unified Einstein radius. This parameter directly quantifies deviations from an isothermal mass profile. We then performed comprehensive statistical analyses, including global distribution characterization, correlation studies with stellar velocity dispersion and redshift, and explicit quantification of systematic biases arising from both inconsistent Einstein angle conventions and survey-specific selection effects.

Our investigation yielded several key physical insights into the properties of early-type galaxies and critically quantified the impact of data heterogeneity:

1. **Average Mass Profiles and Shapes:** For the full homogenized sample, we found that early-type galaxies, on average, exhibit total mass density profiles that are slightly shallower than isothermal, with a mean $f_\sigma = 0.934 \pm 0.176$. Their projected mass distributions are significantly elliptical, with a mean axis ratio $q = 0.770 \pm 0.145$.

2. **The Mass-Structure Relation:** A strong and highly significant positive correlation ($\rho = 0.57, p \ll 0.001$) was found between f_σ and stellar velocity dispersion. This indicates a robust "mass-structure relation," where more massive early-type galaxies tend to possess systematically steeper total mass profiles, closer to or slightly steeper than isothermal. This suggests a mass-dependent interplay between baryonic and dark matter components or assembly history.

3. **No Significant Evolution or Shape-Slope Coupling:** We found no statistically significant evolution of f_σ with lens redshift within our sample ($z_L \approx 0.06 - 1.00$), implying that the inner mass structure of massive ETGs is largely established by $z \approx 1$. Furthermore, no significant correlation was observed between f_σ and the projected axis ratio q, suggesting that the radial mass profile slope is largely independent of the galaxy's projected two-dimensional shape.

4. **Quantified Bias from Einstein Angle Convention:** Our homogenization revealed that failing to correct for the 'Major' axis Einstein angle convention systematically overestimates f_σ by approximately 6.3%. This highlights a crucial source of systematic error that, if unaddressed, could lead to artificially steeper inferred mass profiles.

5. **Quantified Bias from Survey Selection Effects:** We demonstrated that survey selection effects introduce substantial variations (exceeding 10%) in derived parameters between different strong lensing surveys. Notably, ground-based observations showed larger systematic biases and greater scatter compared to space-based data. For instance, some ground-based surveys yielded mean f_σ values deviating by up to +17% from the global average, and mean q values deviating by over -11%. This underscores that observational conditions and selection biases profoundly impact the representativeness and robustness of astrophysical conclusions drawn from heterogeneous samples.

In summary, this study provides robust constraints on the total mass density profiles and shapes of early-type galaxies by meticulously addressing the pervasive issue of data heterogeneity in strong lensing datasets. We have not only characterized the average properties and scaling relations of these galaxies but have also explicitly quantified the systematic biases that can arise from inconsistent parameter definitions and survey selection effects. Our findings underscore the critical importance of careful data homogenization and comprehensive bias quantification for drawing reliable astrophysical conclusions from combined strong lensing observations. This work offers a more accurate picture of the inner mass structure of massive early-type galaxies and sets a precedent for best practices in future strong lensing analyses, paving the way for more precise insights into galaxy formation and evolution.